Published in final edited form as:
J Med Chem. 2012 August 9; 55(15): 6751–6761. doi:10.1021/jm3001218.

Antitumor Agents 295. E-ring Hydroxylated Antofine and Cryptopleurine Analogs as Antiproliferative Agents: Design, Synthesis, and Mechanistic Studies

Xiaoming Yang[†], **Qian Shi**[†,*], **Chin Yu Lai**[⊥], **Chi-Yuan Chen**[§], **Emika Ohkoshi**[†], **Shuenn-Chen Yang**[§], **Chih-Ya Wang**[†], **Kenneth F. Bastow**[‡], **Tian-Shung Wu**[#], **Shiow-Lin Pan**[⊥], **Che-Ming Teng**[⊥], **Pan-Chyr Yang**[⊥,*,§,Ψ], and **Kuo-Hsiung Lee**[†,*,#]

[†]Natural Products Research Laboratories and UNC Eshelman School of Pharmacy, University of North Carolina, Chapel Hill, NC 27599-7568, USA

[‡]Division of Chemical Biology and Medicinal Chemistry, UNC Eshelman School of Pharmacy, University of North Carolina, Chapel Hill, NC 27599-7568, USA

[§]Institute of Biomedical Sciences, Academia Sinica, Taipei, Taiwan

[⊥]Department of Internal Medicine, College of Medicine, and Research Center for Medical Excellence, National Taiwan University, Taichung 404, Taiwan

[Ψ]Division of Genomic Medicine, Research Center for Medical Excellence, National Taiwan University, Taichung 404, Taiwan

[#]Chinese Medicine Research and Development Center, China Medical University and Hospital, Taichung 404, Taiwan

Abstract

Various E-ring hydroxylated antofine and cryptopleurine analogs were designed, synthesized, and tested against five human cancer cell lines. Interesting structure-activity relationship (SAR) correlations were found among these new compounds. The most potent compound **13b** was further tested against a series of non-small cell lung cancer (NSCLC) cell lines, in which it showed impressive antiproliferative activity. Mechanistic studies revealed that **13b** is able to down-regulate HSP90 and β-catenin in A549 lung adenocarcinoma cells in a dose-dependent manner, suggesting a potential use for treating Hedgehog pathway-driven tumorigenesis.

INTRODUCTION

Phenanthroindolizidine and phenanthroquinolizidine alkaloids, well-known for their profound antiproliferative activity, are receiving renewed attention from scientists searching for new cancer drugs with novel mechanism of action. These natural products, represented by tylophorine, antofine, and cryptopleurine, have a common pentacyclic structure with the phenanthrene ring conjugated with the indolizidine or quinolizidine moiety (Figure 1). Their pharmacological use can be traced to ancient times when people used the leaves of these plants to treat inflammation-related diseases, such as asthma, bronchitis, rheumatism, and

[*]**Corresponding Authors** QS. Phone: 919-843-6325. Fax: 919-966-3893. qshi1@email.unc.edu PCY. Phone: 886-2-2356-2185. Fax: 886-2-2322-4793. pcyang@ntu.edu.tw KHL. Phone: 919-962-0066. Fax: 919-966-3893. khlee@unc.edu.

Supporting Information Biological studies and HPLC analysis of final compounds. This material is available free of charge via the Internet at http://pubs.acs.org.

The authors declare no competing financial interest.

dysentery.[1] The NCI cancer drug screening program demonstrated that these natural products generally exhibited significant activity with average IC_{50} values in the low nM range.[2] Other studies suggested that these molecules might act via several mechanisms, possibly different from those of currently launched drugs.[3] Many potential targets have been reported, including inhibition of protein synthesis and ribosomal subunits,[4] inhibition of HIF-1,[5] thymidylate synthase and dihydrofolate reductase,[6] suppression of signaling pathways such as NF-κB, AP-1, and CRE, as well as a number of cell cycle regulatory proteins such as cyclin and cyclin dependent kinases.[3]

However, current research remains largely at bench-side due to the potential CNS toxicity of tylophorine alkaloids, as observed with *R*-tylocrebine in early clinical trials. To circumvent this problem, it was first proposed by Suffness in 1980 that increasing the polarity might potentially reduce such side effects,[7] but until now few efforts have been reported to address this particular issue. A tylophorine analog with a C14 hydroxy group, (13a*S*)-9,11,12,13,13a,14-hexahydro-2,3,6,7-tetramethoxy-dibenzo[*f*,*h*]pyrrolo[1,2-*b*]i soquinolin-14-ol (DCB-3503), showed strong antiproliferative activity *in vivo*, possibly due to an improved bioavailability profile.[8] In addition, phenanthrene-based tylophorine analogs exhibited strong antiproliferative activity both *in vitro* and *in vivo* without any notable toxic effect in a xenograft mouse model of human lung tumor.[9] Interestingly, our group recently established a new synthetic methodology that is able to accommodate numerous E-ring modified analogs from a key intermediate.[10] We designed and synthesized a series of novel analogs by incorporation of an extra heteroatom in the E-ring in order to increase the polarity. Among the synthesized analogs, *S*-13-oxa-cryptopleurine and *S*-13-oxa-E7 exhibited antiproliferative activity *in vitro* with improved cancer cell line selectivity. *In vivo* studies showed that the former compound was active against HT-29 human colorectal adenocarcinoma xenograft in mice, in addition to exhibiting a desirable and expected ten-fold reduction of toxicity against a primary human umbilical vein endothelial cell (HUVEC) line when compared with *R*-cryptopleurine.[11]

Given the promise of our initial findings, we have further designed and synthesized a number of novel E-ring modified compounds, in which a OH group has been introduced at different positions of the E-ring of antofine (compounds **3a**, **3b**, **9a**, and **9b**) and cryptopleurine (**13a**, **13b**, **19a**, **19b**, **21a**, and **21b**). New E-ring dihydroxylated analogs (**24a** and **24b**) of *R*-cryptopleurine, along with other related analogs (**25**, **26a**, and **26b**), have also been prepared and evaluated. These modifications allowed for an enhanced SAR analysis of the effect of introducing polar functionalities. In this paper, we report the design, synthesis, SAR, and mechanistic studies of hydroxylated antofine and cryptopleurine analogs as promising anticancer agents, from which a refined structural design and optimization can be rationalized.

CHEMISTRY

E-ring modifications of *R*-antofine

Compound **1** was prepared according to our published procedures. Following oxidation of the hydroxymethyl group of **1** to an aldehyde, reaction with the enolate of EtOAc gave a pair of diastereomers. Both intermediates underwent cyclization to afford an inseparable mixture of **2a/b** after removal of the Boc group. The resultant amides were reduced to give two C13 hydroxylated target products, 13*S*-hydroxy-*S*-antofine (**3a**) and 13*R*-hydroxy-*S*-antofine(**3b**).

For the synthesis of C12-hydroxyl analogs, compound **4**, obtained from compound **1** by sequential oxidation and Wittig olefination, was condensed with 2-methoxyacrylic acid to form amide **5** after deprotection. E-ring closure then took place through intramolecular ring-

closure metathesis (RCM) using Grubb's catalyst to give compound **6**. Following regioselective reduction to give amine **7,** acid-mediated cleavage of the enol ether furnished ketone **8**. The carbonyl group was reduced by $NaBH_4$ to give the target product 12*R*-hydroxy-*S*-antofine (**9a**) and 12*S*-hydroxy-*S*-antofine (**9b**) (Scheme 2).

E-ring modifications of *R*-cryptopleurine

For the three pairs of cryptopleurine analogs (**13a/13b**, **19a/19b**, **21a/21b**), the hydroxy group was introduced at the C12, C13, and C14 position, respectively.

The known aldehyde **10** was reacted with vinylmagnesium bromide to give a mixture of alcohols, which were oxidized to α,β-unsaturated ketone **11**. The E-ring was then generated through intramolecular Michael addition to give **12** after removal of the Boc group. Subsequently the ketone was reduced using either $NaBH_4$ to give **13a** (13*S*-hydroxy-*S*-cryptopleurine) and **13b**-(13*R*-hydroxy-*S*-cryptopleurine) in a ratio of 3:7 or L-selectride with a higher diastereomeric ratio (*dr*) of 1:9 (Scheme 3). Both compounds could also be synthesized via a similar method as described in Scheme 1 starting from compound **10** in a ratio of about 1:2.

The synthetic approach used to introduce the OH group at the C12 position is illustrated in Scheme 4. Using this strategy, aldehyde **10** was reacted with $Ph_3P{=}CH_2Br$ to produce alkene **14**, which was then coupled with 2-methoxyacrylic acid to give amide **15** after removal of the Boc group. RCM furnished cyclized compound **16** and reduction produced **17**. Hydrolysis of **17** gave the ketone **18**, which was then reduced to alcohols **19a** (12*R*-hydroxy-*R*-cryptopleurine) and **19b** (12*S*-hydroxy-*R*-cryptopleurine) with $NaBH_4$ in a ratio of 4:1. However, only **19a** was isolated when L-selectride was used at a low temperature.

To achieve C14 hydroxylation, compound **1** was oxidized to an aldehyde followed by nucleophilic addition of lithium propiolate prepared *in situ*. The intermediate alcohol mixture was then hydrogenated, and subsequent cyclization afforded an inseparable mixture of **20a**/**20b** after deprotection. ^{1}H-NMR indicated the two diastereomers were present in a ratio of about 1:1. The target compounds 14*S*-hydroxy-*S*-cryptopleurine (**21a**) and 14*R*-hydroxy-*S*-cryptopleurine (**21b**) were then obtained by borane dimethyl sulfide (BMS) reduction (Scheme 5).

Besides E-ring monohydroxylation, other modifications included C12,13-dihydroxylation (Scheme 6) and introduction of various other functionalities at the C13 position of cryptopleurine (Scheme 7).

Compound **10** was converted to *E*)-alkene **22** using $Ph_3P{=}CH_2CO_2Et$. Following dihydroxylation, the intermediate was cyclized to give a mixture of **23a**/**23b** after deprotection. ^{1}H-NMR indicated that the *dr* was about 5:4. The amide was then reduced to afford 12*S*,13*S*-dihydroxy-*S*-cryptopleurine (**24a**) and 12*R*,13*R*-dihydroxy-*S*-cryptopleurine (**24b**) using BMS.

For compound **25**, ketone **12** was treated with EtMgBr, and only one diastereomer was isolated. Because direct methylation of compound **13b** failed to give 13-methoxycryptopleurine **26**, compounds **26a** and **26b** had to be prepared indirectly. Compound **10** was subjected to nucleophilic addition with ethyl acetate using lithium hexamethyldisilazide (LHMDS) followed by cyclization, as for conversion of **1** to **2a**/**2b**. The hydroxy group was then methylated using Me_2SO_4 and NaH, and the amide was reduced by BMS to afford compounds **26a** and **26b**.

The configurations of the new chiral center in compounds **3a**/**3b**, **9a**/**9b**, **13a**/**13b**, **19a**/**19b**, **21a**/**21b**, **24a**/**24b**, and **25** were determined from NOESY spectra. The configurations of **26a** and **26b** were determined to be (13*S*,14a*S*) and (13*R*,14a*S*), respectively, by spectroscopic correlation with compounds **13a** and **13b** (J = 2.8 Hz at C13).

RESULTS AND DISCUSSION

Selected new analogs were tested for antiproliferative activity against a panel of up to five human cancer cell lines from diverse tissue sources, including A549 (lung), DU-145 (prostate), KB (nasopharyngeal), HCT-8 (colon), and SKBR3 (breast); KBvin is a type I multi drug resistant (MDR-1) sub-line of KB that overexpresses P-glycoprotein. Blood-brain penetration was predicted by PreADMET as reported previously.[11]

Regarding the C13-OH derivatives of *R*-antofine, both **3a** and **3b** showed decreased antiproliferative activity (≥ 10 fold) in comparison with *R*-antofine. The 13*R* isomer **3b** exhibited three- to ten-fold higher activity than the 13*S* isomer **3a**, indicating a favored orientation of the OH group at this position. The C12 hydroxylated analogs (**9a**/**9b**) also exhibited reduced activity at a level comparable with the C13 hydroxylated analogs; however, it is still interesting to note that the 12*R* isomer **9a** was about two- to three-fold more active than its 12*S* isomer **9b**. Although generally less active than the natural alkaloid, these new compounds did demonstrate a conformational preference, likely due to increased interaction with their potential targets. Intermediates **7** and **8** were also less active than antofine. The IC_{50} values of compound **8** were similar to those of **9a**, in the medium to high nM range. These studies suggested that the C12 and C13 positions of *R*-antofine might not be suitable for polar modifications, because the measured bioactivity was substantially reduced, even though lowered BBB penetration was predicted.

In this study, we next examined structural optimization of cryptopleurine. The *R*-isomer has shown comprehensive and superior antiproliferative activity with IC_{50} values as low as pM range against all 60 cell lines in the NCI's screening program.[2] With such profound cytotoxicity, substantial activity could be retained even after introduction of polar elements. Based on this line of reasoning, a hydroxy group was introduced at the C12, C13, or C14 position. The IC_{50} data of the mono-hydroxylated cryptopleurine analogs are listed in Table 2.

The results showed that **13a** and **13b** exhibited significant antiproliferative activity. Compound **13b** was at least two-fold more active than **13a** with an average IC_{50} of 20 nM against A549, DU145, KB, and KBvin. Compound **13b** also exerted significant cytotoxic activity against the SKBR3 breast cancer cell line with an IC_{50} of 72 nM, almost four-fold more potent than **13a** (IC_{50} of 295 nM). It is noteworthy that the ketone precursor **12** was also active with an average IC_{50} less than 50 nM against four tested cancer cell lines; the potencies, in general, fell between those of **13a** and **13b**. These data indicated that, for *R*-cryptopleurine, the introduction of OH at C13 position is desirable as discussed above, and therefore, this position may be amenable to further synthetic modification. When the carbonyl group was moved to the C12 position as in compound **18**, the activity was substantially decreased by 15- to 30-fold in comparison with compound **12**. This effect might result from either a conformational mismatch with the putative targets or from the reduced electron density on the N atom, because of the adjacent carbonyl in compound **18**, as it is well known that the C11 amide analogs of these natural products have negligible activity. For **19a** and **19b**, the 12*R*-OH isomer showed considerably higher inhibition *in vitro* (IC_{50} around 30–80 nM, except for SKBR3) than its 12*S*-OH isomer (IC_{50} > 2 μM). The differences between C12-OH isomers were much higher and distinct than those observed with C13-OH derivatives. Again, ketone **18** fell between the two C12-OH isomers

with a potency order of **19a** > **18** > **19b**. The overall potency magnitudes showed that, for *R*-cryptopleurine, the C13 position can more readily tolerate conformational changes, whereas the C12 position is more intolerant of structural alterations, and the spatial orientation of the OH group imposes more substantial effects on potency.

Investigation of C14 hydroxylation of *R*-cryptopleurine gave similar interesting results (Table 2). The 14*S*-OH isomer **21a** exhibited much greater activity than its 14*R*-OH isomer **21b** (average IC_{50} values: 20 nM vs. 200 nM). Therefore, a similar preference for the OH orientation was found with the hydroxylation at both C14 and C12 (the two positions β to the N atom on the E-ring); namely, analogs with the C-O bond *trans* to the C14a-H bond (**19a**, **21a**) had much better antiproliferative activity than their *cis* counterparts (**19b**, **21b**). Among these four analogs, the rank order of potency was **21a** (14*S*-OH) > **19a** (12*R*-OH) > **21b** (14*R*-OH) >> **19b** (12*S*-OH). The data suggest that the OH group might exert smaller steric and electronic differentiating effects at C14 relative to the C12 position. Therefore, the C14 position was shown to be less demanding for modifications than the C12 position. Furthermore, both **21a** and **21b** displayed moderate selectivity against the A549 cell line (10 and 69 nM), which *R*-cryptopleurine did not. All analogs showed remarkably reduced BBB penetration compared with the parent compound as predicted by PreADMET.

Considering the interesting findings resulting from mono-hydroxylation, dihydroxylation at C12 and C13 was investigated. The IC_{50} values are listed in Table 3. While both **24a** and **24b** exhibited low potency compared with the mono-hydroxylated analogs **13b** and **19a**, compound **24a** was significantly more potent than **24b.** The latter result is in good agreement with the SAR relationship established previously, as the two hydroxy groups in **24a** are in the preferred orientations, i.e., those of **13b** (13α OH) and **19a** (12β OH). However, the activity loss could be either target-dependent or possibly related to cell permeability.

Geminal substituents (Et and OH) or a methoxy group were also introduced at the C13 position of *R*-cryptopleurine, and the resulting compounds were tested *in vitro*. The IC_{50} data are shown in Table 4. The antiproliferative activity of analog **13b** was compromised by the introduction of an ethyl group at C13 (**25** exhibited about 40-fold lower activity), which might be caused by steric factors. The effect of introducing a methoxy group at C13 was very interesting, as the two diastereomers **26a** and **26b** showed distinct cell growth inhibition profiles. The 13*R*-OMe isomer **26b** exhibited significant cytotoxicity (average IC_{50} < 100 nM), while the 13*S*-OMe isomer **26a** showed a substantial decrease in efficacy (average IC_{50} > 3 μM). Interestingly, this disparity was not observed between **13a** and **13b**, the corresponding hydroxy analogs of **26a** and **26b**, respectively. In addition, the fact that **26b** was about two-fold less active than **13b**, suggested that group bulkiness or a hydrogen bonding effect may potentially be involved. Overall, the SAR analysis around the C13 position showed that polar substituents *syn* to the C14a-H are favorable for maintaining the high cytoxicity of *R*-cryptopleurine, and OMe versus OH results in decreased potency, but greater stereochemical preference.

In summary, several polar *R*-cryptopleurine analogs, **12**, **13a**, **13b**, **19a**, **21a**, and **26b** that retain significant antiproliferative activity were developed, and new and important SAR information was obtained for each position examined. Because the preliminary cytotoxicity profile indicated some specificity towards the lung cancer cell line A549, selected compounds were evaluated for cytotoxic effect against CL1-5 NSCLC cells through an SRB assay. The results shown in Figure 2 demonstrated that (after the cells were treated with increasing concentration for 48 h), compound **13b** was the most potent inhibitor against CL1-5 cell growth, showing significant cytotoxicity consistent with the earlier study in A549 cells. To explore the effects of **13b** on other NSCLC cells in addition to CL1-5, follow

up assays using CL1-0, PC9, and PC9IR cell lines were conducted, and the cytotoxicity results are shown in Table 5. Compound **13b** strongly inhibited replication of all cell lines, with highest activities against CL1-5, PC9 (~ 8 nM), and A549 (9 nM), while *R*-cryptopleurine showed a uniform higher potency in the same assay. It is exciting and interesting to note that, as compared with cryptopleurine (IC_{50} ~ 14 nM), analog **13b** with a 13*R* hydroxy group exhibited lowered toxicity (IC_{50} ~ 100 nM) against normal human lung fibroblasts, MRC-5, and thus, improved selectivity in this study, (Table 5), while another published analog, *S*-13-oxa-cryptopleurine, exhibited even lower toxicity (IC_{50} ~ 250 nM) against MRC-5 cells. These results demonstrated that our structural modification strategy, namely, the introduction of polar functionalities on the E-ring to reduce potential side effects of this family of natural alkaloids, holds great promise. Compound **13b** was subsequently selected for further molecular cell-based functional study. A549 cells were treated with increasing concentrations of **13b** for 48 h, and morphological observations were captured by using an inverted phase-contrast microscope and photographed. As shown in Figure 3, the number of A549 cells, but not the morphology, was markedly decreased upon treatment with **13b** at 60 nM, suggesting that **13b** significantly inhibits NSCLC proliferation through a mechanism other than morphological effects.

In order to understand the molecular mechanism of **13b**-induced cytotoxicity, a gene expression analysis (MetaCore database) was performed using the A549 cancer cell line. Up- or down-regulated genes in **13b**-treated A549 cells (expression level was 10-fold greater or lower than untreated cells) are summarized in Table 6. Although the microarray used in the current study contained a limited number of genes, we found that genes involved in the Hedgehog signaling pathway exhibited high statistically significant differences (Table 6 and Figure 3), including up-regulation of ubiquitin, and down-regulation of heat shock protein 90 (HSP90) and β-catenin. As many HSP client proteins, such as β-catenin, are known to play critical roles in human cancers, and strategies targeting HSP have been developed for therapeutic applications in human cancers, we focused in particular on the down-regulation of HSP90 and β-catenin in **13b**-treated A549 cells. RT-PCR (Figure 4a) confirmed that both proteins were remarkably decreased after exposure to **13b** (3.6 nM) for 48 h. To further evaluate the significance of these findings, the protein levels of HSP90, p-GSK3β, β-catenin, and β-catenin downstream target genes, such as cyclin D, were determined by Western blot analysis, using *R*-cryptopleurine as a comparison. Similar inhibition patterns were observed with **13b** showing stronger suppression of HSP90 and β-catenin than *R*-cryptopleurine, as opposed to cyclin D (Figure 4b). These findings suggest that **13b** down-regulates HSP90 and β-catenin, which might lead to down-regulation of cyclin D (a common key effector) as proposed in Figure 5. However, it should not be ruled out that the reduction of other RNAs and associated protein levels, if any, might also contribute to the observed potent cytotoxicity of cryptopleurine and related analogs described herein. Several lines of evidence indicate functional interactions between two critical pathways, SHH (sonic hedgehog) and Wnt/β-catenin. It has been recently reported that Wnt/β-catenin signaling is required for Hedgehog pathway-driven tumorigenesis.[12] Therefore, it might be very important to block Wnt signaling, given its activation in NSCLCs. In addition, HSP90, the signal transduction chaperone, maintains intracellular communication in normal, stem, and cancer cells. The well-characterized associations of HSP90 with its client kinases form the framework of multiple signaling networks. Recently, HSP90 has emerged as a target of interest in cancer therapy. Moreover, evidence also suggests that the β-catenin/TCF7L2 pathway plays an important role in HSP90 inhibitor-induced cell death in ATL cells (adult T-cell leukemia) and HTLV-1 (human T-cell leukemia virus type 1) transformed cells,[13] and HSP90 co-localizes with GSK3β and β-catenin in the human MCF-7 epithelial breast cancer model. These data indicate that β-catenin could be considered as a novel HSP90 client protein. However, the proposed

mechanism in Figure 5 still needs further direct evidence, as some of the gene expressions were validated only at RNA levels, which do not necessarily translate into protein levels. In addition, the degree of HSP90 involvement in Wnt/β-catenin signaling and the role of **13b** in the complex merit further investigation.

CONCLUSION

In this paper, we designed and synthesized novel polar antofine and cryptopleurine analogs. Several analogs exhibited significant inhibition of cancer cell growth *in vitro*, and a detailed SAR discussion was provided. The higher polarity of these new analogs could potentially reduce CNS toxicity, a major drawback of the natural phenanthroindolizidines and phenanthroquinolizidines. Mechanistic studies suggested that these new analogs interact with the Hedgehog signaling pathway to exert their profound cytotoxicity, probably by inhibiting HPS90 or β-catenin activity, as demonstrated by cDNA microarray analysis. Therefore, these compounds could potentially be useful in treating HSP90- or β-catenin-related carcinogenesis. Similar structural modifications are being studied with another member of this alkaloid family, tylophorine. Additional mechanistic studies are still underway, and the results will be reported in due course.

EXPERIMENTAL SECTION

All chemicals were used as purchased. Melting points were measured using a Fisher Johns melting apparatus without correction. Proton nuclear magnetic resonance (^{1}H NMR) spectra were measured on a 300 MHz Gemini or a Varian Inova (400 MHz) NMR spectrometer with TMS as the internal standard. The solvent used was $CDCl_3$ unless otherwise indicated. Mass spectra were recorded on a Shimazu-2010 LC/MS/MS instrument equipped with a TurboIonsSpray ion source. All final target compounds were characterized and determined as at least >95% pure by analytical HPLC.

(13*R*/*S*,13a*S*)-11-Oxo-13-hydroxyantofine (2a/2b)

Alcohol **1** (113 mg, 0.25 mmol) was dissolved in CH_2Cl_2 (10 mL) and Et_3N (0.14 mL, 1 mmol), to which sulfur trioxide pyridine complex (Py•SO_3) (120 mg, 0.75 mmol) in DMSO was added dropwise. The mixture was stirred for 1.5 h, and then 1N HCl was added. The organic layer was washed with sat. $NaHCO_3$ and brine, and dried over $MgSO_4$. In another flask, ethyl acetate (30 μL, 0.30 mmol) was added to lithium bis(trimethylsilyl)amide (LiHMDS) (0.33 mmol) in THF at −78 °C with stirring for 1h, and the aldehyde from the first reaction was added slowly in THF. The mixture was stirred for 3 h until TLC indicated complete disappearance of the aldehyde. Sat. NH_4Cl was added to quench the reaction, and most of the solvent was removed in vacuo. CH_2Cl_2 was added and the organic layer was washed with sat. $NaHCO_3$ and brine, and dried over Na_2SO_4. After evaporation of solvent, the residue was dissolved in TFA/CH_2Cl_2, and stirred for 1 h. After removal of TFA in vacuo, Et_3N (0.20 mL) and MeOH (10 mL) were added. The mixture was refluxed for 1 h. Chromatography using CH_2Cl_2/MeOH gave 56 mg (57% over four steps) of an inseparable mixture of **2a/2b** in a ratio of 2:1 as a white solid. ^{1}H NMR (400 MHz, $CDCl_3$): δ 7.87 (s, 1H), 7.85 (d, *J* = 2.4 Hz, 1H), 7.80 (d, *J* = 9.2 Hz, 1H), 7.63 (s, 0.5H), 7.54 (d, *J* = 2.4 Hz, 0.52H), 7.31 (d, *J* = 8.8 Hz, 0.55 H), 7.22–7.19 (m, 2H), 7.15 (s, 0.51H), 6.76 (dd, *J* = 9.2 Hz, *J* = 2.4 Hz, 0.52H), 5.38 (d, *J* = 17.2 Hz, 1H), 4.93 (d, *J* = 17.6 Hz, 0.56 H), 4.66 (m, 0.58 H), 4.57 (d, *J* = 17.2 Hz, 1H), 4.51 (m, 1H), 4.40 (d, *J* = 17.6 Hz, 0.59H), 4.11 (s, 4.23H), 4.04 (s, 4.25H), 4.01 (s, 2.79H), 3.90 (s, 1.49H), 3.85–3.75 (m, 1.69 H), 3.51 (dd, *J* = 15.6 Hz, *J* = 4.0 Hz, 1H), 3.40 (dd, *J* = 16.0 Hz, *J* = 11.2 Hz, 0.64H), 3.18–3.09 (m, 1.24H), 2.94 (dd, *J* = 17.6 Hz, *J* = 7.2 Hz, 1H), 2.88 (dd, *J* = 6.4 Hz, *J* = 17.6 Hz, 0.50H), 2.74 (dd, *J* = 15.2 Hz, *J* = 11.2 Hz, 1H), 2.66 (d, *J* = 18.0 Hz, 0.60H), 2.59 (dd, *J* = 17.6 Hz,

J = 2.4 Hz, 1H); ESI MS *m/z* 394.10 $(M+H)^+$. ESI-HRMS ($[M + H]^+$) calcd for $C_{23}H_{23}NO_5$ 394.1654, found 394.1660.

(13*S*,13a*S*)-13-Hydroxyantofine (3a) and (13*R*,13a*S*)-13-hydroxyantofine (3b)

Compound **2a**/**2b** (56 mg) was suspended in THF and $LiAlH_4$ (20 mg, 0.50 mmol) was added. The mixture was stirred at rt for 1 h. Water and 1N NaOH were then added and the mixture was filtered. CH_2Cl_2 was used for extraction in a normal workup. Chromatography using CH_2Cl_2/MeOH gave 27 mg of **3a** (48%) and 12 mg (22%) of **3b** as white solids. For **3a**: mp 170–172 °C; $[\alpha]^{23}_D$= −7.3 ° (*c* 0.83, $CHCl_3$); ^{1}H NMR (400 MHz, $CDCl_3$): δ 7.88 (d, *J* = 2.8 Hz, 1H), 7.79 (s, 1H), 7.76 (d, *J* = 9.2 Hz, 1H), 7.17 (dd, *J* = 9.2 Hz, *J* = 2.4 Hz, 1H), 6.77 (s, 1H), 4.67 (d, *J* = 14.8 Hz, 1H), 4.32 (m, 1H), 4.10 (s, 3H), 4.02 (s, 3H), 3.66 (s, 3H), 3.58 (d, *J* = 15.2 Hz, 1H), 3.51 (dt, *J* = 8.8 Hz, *J* = 2.4 Hz, 1H), 3.11 (dd, *J* = 16.0 Hz, *J* = 11.2 Hz, 1H), 2.93 (dd, *J* = 16.0 Hz, *J* = 3.2 Hz, 1H), 2.46–2.40 (m, 1H), 2.36–2.26 (m, 2H), 1.93–1.88 (m, 1H); ESI-HRMS ($[M + H]^+$) calcd for $C_{23}H_{25}NO_4$ 380.1862, found 380.1858. For **3b**: mp 182–184 °C; $[\alpha]^{23}_D$= −92.2 ° (*c* 0.18, $CHCl_3$); ^{1}H NMR (400 MHz, $CDCl_3$): δ 7.88–7.87 (m, 2H), 7.77 (d, *J* = 9.2 Hz, 1H), 7.29 (s, 1H), 7.19 (dd, *J* = 9.2 Hz, *J* = 2.4 Hz, 1H), 4.58 (d, *J* = 15.2 Hz, 1H), 4.35–4.30 (m, 1H), 4.09 (s, 3H), 4.04 (s, 3H), 4.01 (s, 3H), 3.74 (d, *J* = 14.8 Hz, 1H), 3.47 (dd, *J* = 15.6 Hz, *J* = 2.8 Hz, 1H), 3.37 (dt, *J* = 8.8 Hz, *J* = 2.4 Hz, 1H), 2.96 (dd, *J* = 15.2 Hz, *J* = 11.2 Hz, 1H), 2.72 (q, *J* = 9.2 Hz, 1H), 2.50–2.44 (m, 2H), 1.83–1.76 (m, 1H); ESI-HRMS ($[M + H]^+$) calcd for $C_{23}H_{25}NO_4$ 380.1862, found 380.1865.

(*S*)-*N*-2'-Methoxypropenoyl-6,7,10-trimethoxy-3-vinyl-1,3,4-trihydrodibenzo[*f*,*h*]-isoquinoline (5)

Compound **4** (900 mg, 2 mmol) was dissolved in TFA/CH_2Cl_2 (20 mL) at rt, and the mixture was stirred for 1 h. The solvent was removed by evaporation and TFA was neutralized with *N*-methylmorpholine (NMM). The residue was redissolved in DMF (20 mL), to which 2-methoxyacrylic acid (224 mg, 2.20 mmol), 1-ethyl-3-(3-dimethyllaminopropyl)carbodiimide hydrochloride (EDC•HCl) (478 mg, 2.50 mmol), hydroxybenzotriazole (HOBt) (340 mg, 2.50 mmol), and NMM (0.80 mL) were added. Stirring was continued overnight. DMF was then removed under reduced pressure, and the residue was dissolved in CH_2Cl_2 (50 mL), washed with HCl (1N), sat. $NaHCO_3$, and brine, and dried over $MgSO_4$. Compound **5** (727 mg, 83% in two steps) was isolated by column chromatography eluting with EtOAc/hexane. mp 74–76 °C; $[\alpha]^{23}_D$= 71.5 ° (*c* 1.16, $CHCl_3$); ^{1}H NMR (400 MHz, $CDCl_3$, compound rotameric at rt): δ 7.89–7.84 (m, 3H), 7.28 (s, 1H), 7.21 (dd, *J* = 9.2 Hz, *J* = 2.8 Hz, 1H), 5.88–5.61 (m, 2H), 5.20–5.10 (m, 3H), 4.64 (d, *J* = 3.2 Hz, 1H), 4.54 (m, 1H), 4.46 (d, *J* = 3.2 Hz), 4.09 (s, 3H), 4.05 (s, 3H), 4.00 (s, 3H), 3.73 (s, 3H), 3.43–3.28 (m, 2H); ^{13}C NMR (100 MHz, $CDCl_3$): δ 165.9, 162.6, 157.9, 157.2, 149.7, 148.8, 135.9, 130.4, 126.5, 124.3, 123.8, 123.7, 123.3, 117.7, 115.2, 105.0, 104.1, 103.9, 56.1, 56.0, 55.6, 55.3, 53.8, 39.6, 36.5, 31.5, 30.3; ESI-HRMS ($[M + H]^+$) calcd for $C_{26}H_{27}NO_5$ 434.1967, found 434.1963.

(*S*)-11-Oxo-12-methoxy-antofine-12-ene (6)

Compound **5** (727mg, 1.66 mmol) was dissolved in anhydrous CH_2Cl_2 under N_2, to which Grubb's 2nd generation catalyst in CH_2Cl_2 was added in one portion. The reaction was stirred at reflux for 2 h or monitored by TLC. Compound **6** (596 mg) was isolated by column chromatography eluting with CH_2Cl_2/MeOH as a light yellow solid. Yield: 88%. mp 135–137 °C; $[\alpha]^{23}_D$= −235 ° (*c* 1.11, $CHCl_3$); ^{1}H NMR (400 MHz, $CDCl_3$): δ 7.80 (s, 1H), 7.79 (d, *J* = 2.8 Hz, 1H), 7.72 (d, *J* = 8.8 Hz, 1H), 7.20–7.17 (m, 2H), 6.00 (d, *J* = 2.4 Hz, 1H), 5.37 (d, *J* = 17.6 Hz, 1H), 4.65 (d, *J* = 17.2 Hz, 1H), 4.16–4.12 (m, 1H), 4.10 (s, 3H), 4.03 (s, 3H), 4.00 (s, 3H), 3.86 (s, 3H), 3.52 (dd, *J* = 11.6 Hz, *J* = 4.8 Hz, 1H), 2.53 (dd, *J* =

15.6 Hz, *J* = 11.6 Hz, 1H); ^{13}C NMR (100 MHz, $CDCl_3$): δ 163.9, 158.0, 153.1, 149.5, 148.7, 130.4, 126.0, 124.1, 124.0, 123.2, 123.2, 122.4, 115.3, 108.7, 104.9, 104.0, 103.9, 57.5, 56.1, 56.0, 55.6, 52.4, 40.4, 31.4; ESI-HRMS ($[M + H]^+$) calcd for $C_{24}H_{23}NO_5$ 406.1654, found 406.1667.

(*S*)-12-Methoxyantofine-12-ene (7)

The amide **6** (450 mg, 1.11 mmol) and $LiAlH_4$ (2 equiv.) were suspended in THF (15 mL), which was stirred for 2 h. Water was then added to quench the reaction, followed by aq. NaOH (1N, 1 mL) and H_2O (1 mL). The mixture was filtered and then extracted with $CHCl_3$ and dried over $MgSO_4$. Column chromatography eluting with CH_2Cl_2/MeOH gave the target product **7** (300 mg) as a light yellow solid. Yield: 69%. mp 202–204 °C; $[\alpha]^{23}_D$= 97.0 ° (*c* 0.47, $CHCl_3$); ^{1}H NMR (400 MHz, $CDCl_3$): δ 7.91 (s, 1H), 7.90 (d, *J* = 2.4 Hz, 1H), 7.80 (d, *J* = 8.8 Hz, 1H), 7.33 (s, 1H), 7.20 (dd, *J* = 9.2 Hz, *J* = 2.4 Hz, 1H), 4.83 (s, 1H), 4.52 (d, *J* = 14.4 Hz, 1H), 4.10 (s, 3H), 4.06 (s, 3H), 4.05 (d, *J* = 14.4 Hz, 1H), 4.01 (s, 3H), 3.83 (d, *J* = 7.2 Hz, 1H), 3.72 (s, 3H), 3.58 (m, 2H), 3.32 (d, *J* = 15.2 Hz, 1H), 3.02 (m, 1H); ^{13}C NMR (100 MHz, $CDCl_3$): δ 159.7, 157.7, 149.6, 148.6, 130.2, 127.7, 127.6, 125.8, 124.5, 124.4, 123.7, 115.1, 104.8, 104.3, 104.0, 95.3, 63.7, 57.8, 57.0, 56.2, 56.0, 55.7, 51.8, 33.8; ESI-HRMS ($[M + H]^+$) calcd for $C_{24}H_{25}NO_4$ 392.1862, found 392.1865.

(*S*)-12-Oxo-antofine (8)

Compound **7** (300 mg) was refluxed in HCl/THF for 2 h before the solvent was evaporated. NaOH was used for neutralization and CH_2Cl_2 used for extraction. Chromatography gave 200 mg of compound **8** as a light yellow solid (68%). mp 240–242 °C; $[\alpha]^{23}_D$= −34.7 ° (*c* 0.91, $CHCl_3$); IR (FT-IR ATR, cm^{-1}) 2833, 1751, 1609, 1510, 1260, 1234, 1208, 1202, 1126, 867, 777; ^{1}H NMR (400 MHz, $CDCl_3$): δ 7.92 (s, 1H), 7.91 (d, *J* = 2.4 Hz, 1H), 7.78 (d, *J* = 8.8 Hz, 1H), 7.27 (s, 1H), 7.22 (dd, *J* = 9.2 Hz, *J* = 2.6 Hz, 1H), 4.70 (d, *J* = 14.8 Hz, 1H), 4.11 (s, 3H), 4.06 (s, 3H), 4.02 (s, 3H), 3.84 (d, *J* = 15.2 Hz, 1H), 3.78 (d, *J* = 16.8 Hz, 1H), 3.43 (d, *J* = 13.2 Hz, 1H), 3.07–3.01 (m, 2H), 2.98 (d, *J* = 16.4 Hz, 1H), 2.76 (dd, *J* = 17.6 Hz, *J* = 5.2 Hz, 1H), 2.43 (dd, *J* = 17.6 Hz, *J* = 10.0 Hz, 1H); ^{13}C NMR (100 MHz, $CDCl_3$): δ 212.4, 157.7, 149.5, 148.6, 130.2, 126.6, 125.7, 124.5, 124.0, 123.7, 123.6, 115.1, 104.7, 103.8, 103.7, 63.1, 57.9, 56.0, 55.9, 53.4, 44.7, 33.2; ESI-HRMS ($[M + H]^+$) calcd for $C_{23}H_{23}NO_4$ 378.1705, found 378.1704.

(12*R*,13a*S*)-12-Hydroxyantofine (9a) and (12*S*,13a*S*)-12-hydroxyantofine (9b)

The ketone **8** (38 mg, 0.10 mmol) was suspended in MeOH, to which $NaBH_4$ (19 mg, 0.50 mmol) was added at r.t. The mixture was stirred for 1 h before sat. $NaHCO_3$ was added. After normal workup, chromatography using MeOH/CH_2Cl_2 gave 19 mg of **9a** (50%) and 12 mg of **9b** (31%) as white solids. For **9a**: mp 235 °C (dec.); $[\alpha]^{23}_D$= −104.5 ° (*c* 0.20, $CHCl_3$); ^{1}H NMR (400 MHz, $CDCl_3$): δ 7.85 (s, 2H), 7.69 (d, *J* = 9.2 Hz, 1H), 7.18 (s, 1H), 7.12 (dd, *J* = 9.2 Hz, *J* = 2.4 Hz, 1H), 4.57 (d, *J* = 14.8 Hz, 1H), 4.41 (m, 1H), 4.09 (s, 3H), 3.99 (s, 6H), 3.57 (d, *J* = 14.8 Hz, 1H), 3.33 (d, *J* = 10.4 Hz, 1H), 3.26 (dd, *J* = 15.6 Hz, *J* = 2.8 Hz, 1H), 2.88 (dd, *J* = 15.2 Hz, *J* = 10.8 Hz, 1H), 2.75–2.68 (m, 1H), 2.54–2.50 (m, 1H), 2.42–2.38 (m, 1H), 1.74–1.68 (m, 1H); ESI-HRMS ($[M + H]^+$) calcd for $C_{23}H_{25}NO_4$ 380.1862, found 380.1866. For **9b**: mp 250 °C (dec.); $[\alpha]^{23}_D$= 19.5 ° (*c* 0.12, $CHCl_3$); ^{1}H NMR (400 MHz, $CDCl_3$): δ 7.92 (s, 1H), 7.90 (d, *J* = 2.4 Hz, 1H), 7.80 (d, *J* = 9.2 Hz, 1H), 7.30 (s, 1H), 7.21 (dd, *J* = 9.2 Hz, *J* = 2.8 Hz, 1H), 4.65 (m, 1H), 4.63 (d, *J* = 14.8 Hz, 1H), 4.11 (s, 3H), 4.06 (s, 3H), 4.02 (s, 3H), 3.86–3.80 (m, 2H), 3.41 (m, 1H), 3.35 (d, *J* = 14.8 Hz, 1H), 2.95–2.83 (m, 2H), 2.49 (dd, *J* = 10.0 Hz, *J* = 4.8 Hz, 1H), 2.20–2.05 (m, 2H); ESI-HRMS ($[M + H]^+$) calcd for $C_{23}H_{25}NO_4$ 380.1862, found 380.1861.

(*S*)-*N*-Boc-6,7,10-trimethoxy-3-vinylcarbonylmethyl-1,3,4-trihydrodibenzo[*f*,*h*] isoquinoline (11)

Compound **10** (700 mg, 1.50 mmol) was dissolved in THF (20 mL), to which vinylmagnesium bromide (3.50 mL, 3.50 mmol) was added dropwise at 0 °C. After 2 h of stirring, sat. NH_4Cl was added to quench the reaction and the mixture was extracted with CH_2Cl_2. The organic layer was washed with aq. $NaHCO_3$ and brine. After drying over Na_2SO_4, the mixture was evaporated and the residue was redissolved in anhydrous CH_2Cl_2. Dess-Martine periodinane (848 mg, 2 mmol) was added and the reaction mixture was stirred for 4 h. $Na_2S_2O_3$ (500 mg) was added followed by sat. $NaHCO_3$, and the mixture was stirred for 10 min. The mixture was extracted with CH_2Cl_2 and the organic layers were combined, washed with brine, and dried over $MgSO_4$. The solvent was removed and the crude was chromatographed using EtOAc/hexane to give **11** (434 mg, 57%) as a light yellow foam. mp 156–158 °C; $[\alpha]^{23}_D$= 111.8 ° (*c* 0.11, $CHCl_3$); ^{1}H NMR (400 MHz, $CDCl_3$, peak broadened due to rotamers at r.t.): δ 7.87 (brs, 3H), 7.22 (brs, 2H), 6.30 (dd, *J* = 17.2 Hz, *J* = 10.4 Hz, 1H), 6.13 (d, *J* = 17.6 Hz, 1H), 5.77 (d, *J* = 6.8 Hz, 1H), 5.27 (m, 2H), 4.61 (m, 1H), 4.08 (s, 3H), 4.02 (s, 3H), 4.00 (s, 3H), 3.32 (dd, *J* = 16.4 Hz, *J* = 6.0 Hz, 1H), 3.15 (brs, 1H), 2.85–2.75 (m, 2H), 1.53 (s, 9H); ESI-HRMS ($[M + H]^+$) calcd for $C_{29}H_{33}NO_6$ 492.2386, found 492.2372.

(*S*)-13-Oxo-cryptopleurine (12)

To a solution of compound **11** (245 mg, 0.50 mmol)in CH_3CN (50 ml) at 0 °C was added TMSI dropwise (3 equiv.). The mixture was stirred for 15 min before the solvent was removed. Then the residue was dissolved in CH_2Cl_2 (5 mL) and MeOH (20 mL), to which Cs_2CO_3 (326 mg, 1 mmol) was added in one portion. The mixture was refluxed overnight. After evaporation of the solvent, the crude product was chromatographed using CH_2Cl_2/MeOH to afford **12** (123 mg, 63%) as a light yellow solid. mp 113–115 °C; $[\alpha]^{23}_D$= 103.9 ° (*c* 0.12, $CHCl_3$); ^{1}H NMR (400 MHz, $CDCl_3$): δ 7.81–7.80 (m, 2H), 7.68 (d, *J* = 9.2 Hz, 1H), 7.16 (dd, *J* = 8.8 Hz, *J* = 2.4 Hz, 1H), 7.04 (s, 1H), 4.42 (d, *J* = 15.6 Hz, 1H), 4.06 (s, 3H), 4.00 (s, 3H), 3.98 (s, 3H), 3.54 (dd, *J* = 15.6 Hz, 1H), 3.43–3.38 (m, 1H), 2.87 (dd, *J* = 16.0 Hz, *J* = 3.2 Hz, 1H), 2.81–2.73 (m, 2H), 2.61–2.40 (m, 5H); ESI-HRMS ($[M + H]^+$) calcd for $C_{24}H_{25}NO_4$ 392.1862, found 392.1856.

(13*S*,14a*S*)-13-Hydroxycryptopleurine (13a) and (13*R*,14a*S*)-13-hydroxycryptopleurine (13b)

To a solution of compound **12** (39 mg, 0.10 mmol) in MeOH was added $NaBH_4$ (19 mg, 0.50 mmol). The reaction mixture was stirred for 2 h before sat. $NaHCO_3$ was added. The mixture was then extracted using CH_2Cl_2 and the organic layers were washed with brine and dried over Na_2SO_4. The crude product was chromatographed using MeOH/CH_2Cl_2 to give **13a** (9 mg, 24%) and **13b** as white solids (21 mg, 55%). The diastereoselectivity was further increased using L-selectride in THF at −78 °C to give **13a**/**13b** in a ratio of 1/9. For **13a**: mp 222 °C (dec.); $[\alpha]^{23}_D$= −95.4 ° (*c* 0.11, $CHCl_3$); ^{1}H NMR (300 MHz, $CDCl_3$): δ 7.89–7.88 (m, 2H), 7.75 (d, *J* = 9.0 Hz, 1H), 7.34 (s, 1H), 7.20 (dd, *J* = 9.0 Hz, *J* = 2.1 Hz, 1H), 4.43 (d, *J* = 15.6 Hz, 1H), 4.07 (s, 3H), 4.04 (s, 3H), 3.99 (s, 3H), 3.69 (m, 1H), 3.54 (d, *J* = 15.6 Hz, 1H), 3.26 (m, 1H), 3.02 (m, 1H), 2.89 (m, 1H), 2.42–2.59 (m, 3H), 2.07 (m, 1H), 1.72 (m, 1H); ESI-HRMS ($[M + H]^+$) calcd for $C_{24}H_{27}NO_4$ 394.2018, found 394.2020. For **13b**: mp 230 °C (dec.); $[\alpha]^{23}_D$= −144.7 ° (*c* 0.10, $CHCl_3$); ^{1}H NMR (300 MHz, $CDCl_3$): δ 7.90 (s, 1H), 7.89 (d, *J* = 2.7 Hz, 1H), 7.80 (d, *J* = 9.0 Hz, 1H), 7.23 (s, 1H), 7.19 (dd, *J* = 9.0 Hz, *J* = 2.4 Hz, 1H), 4.46 (d, *J* = 15.6 Hz, 1H), 4.29 (m, 1H), 4.10 (s, 3H), 4.05 (s, 3H), 4.01 (s, 3H), 3.72 (d, *J* = 15.3 Hz, 1H), 3.08–3.04 (m, 2H), 2.86–2.72 (m, 2H), 2.15–2.03 (m, 2H), 1.90–1.74 (m, 2H); ESI-HRMS ($[M + H]^+$) calcd for $C_{24}H_{27}NO_4$ 394.2018, found 394.2019.

(*S*)-*N*-Boc-6,7,10-trimethoxy-3-(3'-propenyl)-1,3,4-trihydrodibenzo[*f*,*h*]isoquinoli ne (14)

To a solution of $Ph_3P{=}CH_2Br$ (1.43 g, 4 mmol) in THF was added *n*-BuLi (2M in heptanes, 1.95 mL) at 0 °C under N_2. The mixture was stirred for 0.5 h before compound **8** (970 mg, 2.08 mmol) in THF (10 mL) was added dropwise. The mixture was then stirred for 2 h (monitored by TLC). Sat. NH_4Cl was added to quench the reaction and THF was removed by evaporation. The residue was dissolved in CH_2Cl_2, washed with sat. $NaHCO_3$ and brine, and dried over $MgSO_4$. Column chromatography eluting with EtOAc/hexane gave **9** (820 mg, 85%) as a light yellow foam. mp 87–89 °C; $[\alpha]^{23}_D$= 132.7 ° (*c* 0.15, $CHCl_3$); ^{1}H NMR (400 MHz, $CDCl_3$, peak broadened due to rotamers at r.t.): δ 7.92–7.87 (m, 3H), 7.277.23 (m, 2H), 5.89–5.83 (m, 1H), 5.34 (brs, 1H), 5.05–4.79 (m, 3H), 4.53 (d, *J* = 17.2 Hz, 1H), 4.11 (s, 3H), 4.04 (s, 3H), 4.02 (s, 3H), 3.26 (dd, *J* = 16.0 Hz, *J* = 2.0 Hz, 1H), 3.10 (d, *J* = 16.4 Hz, 1H), 2.41–2.33 (m, 1H), 2.21–2.18 (m, 1H), 1.54 (s, 9H); ESI-HRMS ($[M + H]^+$) calcd for $C_{28}H_{33}NO_5$ 464.2437, found 464.2440.

(*S*)-*N*-2'-Methoxypropenoyl-6,7,10-trimethoxy-3-(3'-propenyl)-1,3,4-trihydrodib e-nzo[*f*,*h*]-isoquinoline (15)

Similar procedure as for compound **5**. Yield: 77% over two steps. mp 84–86 °C; $[\alpha]^{23}_D$= 104.9 ° (*c* 4.30, $CHCl_3$); ^{1}H NMR (400 MHz, $CDCl_3$, peak broadened due to rotamers at r.t.): δ 7.93–7.70 (m, 3H), 7.25–7.22 (m, 2H), 5.84–5.76 (m, 1H), 5.68 (d, *J* = 18.0 Hz, 1H), 5.34–5.16 (m, 0.65H), 5.07 (d, *J* = 10.4 Hz, 1H), 5.01 (d, *J* = 17.2 Hz, 1H), 4.77 (d, *J* = 16.8 Hz, 0.29H), 4.61–4.40 (m, 3H), 4.10 (s, 3H), 4.04 (s, 3H), 4.01 (s, 3H), 3.31 (dd, *J* = 16.0 Hz, *J* = 4.8 Hz, 1H), 3.14 (d, *J* = 15.6 Hz, 1H), 2.48–2.41 (m, 1H), 2.29–2.25 (m, 1H); ESI-HRMS ($[M + H]^+$) calcd for $C_{27}H_{29}NO_5$ 448.2124, found 448.2121.

(*R*)-11-Oxo-12-methoxycryptopleurine-12-ene (16)

Similar procedure as for compound **6**. Yield: 65%. mp 276–278 °C; $[\alpha]^{23}_D$= 246.0 ° (*c* 0.16, $CHCl_3$); ^{1}H NMR (400 MHz, $CDCl_3$): δ 7.89 (d, *J* = 8.8 Hz, 1H), 7.85 (s, 1H), 7.84 (d, *J* = 2.4 Hz, 1H), 7.22 (dd, *J* = 9.2 Hz, *J* = 2.4 Hz, 1H), 7.16 (s, 1H), 5.73 (d, *J* = 17.2 Hz, 1H), 5.38 (t, *J* = 4.8 Hz, 1H), 4.62 (d, *J* = 17.2 Hz, 1H), 4.16–4.12 (m, 1H), 4.08 (s, 3H), 4.03 (s, 3H), 4.00 (s, 3H), 3.95–3.90 (m, 1H), 3.66 (s, 3H), 3.24 (dd, *J* = 16.0 Hz, *J* = 11.6 Hz, 1H), 3.00 (dd, *J* = 16.0 Hz, *J* = 2.8 Hz, 1H), 2.94 (ddd, *J* = 17.2 Hz, *J* = 8.0 Hz, *J* = 4.0 Hz, 1H), 2.52 (dt, *J* = 17.2 Hz, *J* = 5.2 Hz, 1H); ESI-HRMS ($[M + H]^+$) calcd for $C_{25}H_{25}NO_5$ 420.1811, found 420.1826.

(*R*)-12-Methoxycryptopleurine-12-ene (17)

Similar procedure as for compound **7**. Yield: 70%. mp 213–215 °C; $[\alpha]^{23}_D$= 17.3 ° (*c* 0.10, $CHCl_3$); ^{1}H NMR (400 MHz, $CDCl_3$): δ 7.90 (s, 1H), 7.89 (d, *J* = 2.4 Hz, 1H), 7.79 (d, *J* = 9.2 Hz, 1H), 7.26 (s, 1H), 7.19 (dd, *J* = 9.2 Hz, *J* = 2.4 Hz, 1H), 4.71 (m, 1H), 4.47 (d, *J* = 16.0 Hz, 1H), 4.10 (s, 3H), 4.06 (d, *J* = 16.0 Hz, 1H), 4.05 (s, 3H), 4.00 (s, 3H), 3.58 (s, 3H), 3.44 (d, *J* = 16.0 Hz, 1H), 3.28 (dd, *J* = 15.6 Hz, *J* = 1.6 Hz, 1H), 3.21–3.14 (m, 2H), 3.00–2.94 (m, 1H), 2.49–2.45 (m, 1H), 2.33–2.27 (m, 1H); ESI-HRMS ($[M + H]^+$) calcd for $C_{25}H_{27}NO_4$ 406.2018, found 406.2030.

(*R*)-12-Oxo-cryptopleurine (18)

Similar procedure as for compound **8**. Yield: 80%. mp 96–98 °C; $[\alpha]^{23}_D$= 82.4 ° (*c* 0.15, $CHCl_3$); ^{1}H NMR (400 MHz, $CDCl_3$): δ 7.90 (s, 1H), 7.89 (d, *J* = 2.4 Hz, 1H), 7.73 (d, *J* = 9.2 Hz, 1H), 7.22 (s, 1H), 7.19 (dd, *J* = 9.2 Hz, *J* = 2.4 Hz, 1H), 4.38 (d, *J* = 15.6 Hz, 1H), 4.10 (s, 3H), 4.05 (s, 3H), 4.01 (s, 3H), 3.75 (d, *J* = 15.6 Hz, 1H), 3.63 (dd, *J* = 14.8 Hz, *J* = 1.2 Hz, 1H), 3.19 (dd, *J* = 16.0 Hz, *J* = 2.4 Hz, 1H), 3.10 (d, *J* = 14.8 Hz, 1H), 2.93 (dd, *J* = 16.0 Hz, *J* = 10.0 Hz, 1H), 2.87–2.82 (m, 1H), 2.68–2.63 (m, 1H), 2.52–2.44 (m, 1H), 2.36–

2.29 (m, 1H), 2.00–1.91 (m, 1H); ESI-HRMS ([M + H]$^+$) calcd for $C_{24}H_{25}NO_4$ 392.1862, found 392.1859.

(12*R*,14a*R*)-12-Hydroxy-cryptopleurine (19a) and (12*S*,14a*R*)-12-hydroxy--cryptopleurine (19b)

The ketone **18** (39 mg, 0.10 mmol) was suspended in MeOH, to which $NaBH_4$ (19 mg, 0.50 mmol) was added at rt. The mixture was stirred for 1 h before sat. $NaHCO_3$ was added. After normal workup, chromatography using MeOH/CH_2Cl_2 gave 23 mg of **19a** (58%) and 6 mg of **9b** (15%) as white solids. The reaction was also performed with L-selectride at 0 °C and only **19a** was isolated (31 mg, 80%). For **19a**: mp 206 °C (dec.); $[\alpha]^{23}_D$= −61.0 ° (*c* 0.13, $CHCl_3$); ^{1}H NMR (400 MHz, $CDCl_3$): δ 7.89 (s, 1H), 7.88 (d, *J* = 2.8 Hz, 1H), 7.76 (d, *J* = 8.8 Hz, 1H), 7.23 (s, 1H), 7.20 (dd, *J* = 9.2 Hz, *J* = 2.4 Hz, 1H), 4.40 (d, *J* = 15.2 Hz, 1H), 4.09 (s, 3H), 4.05 (s, 3H), 4.00 (s, 3H), 3.98–3.91 (m, 1H), 3.66 (d, *J* = 15.2 Hz, 1H), 3.41–3.37 (m, 1H), 3.10 (dd, *J* = 16.4 Hz, *J* = 3.2 Hz, 1H), 2.82 (dd, *J* = 16.4 Hz, *J* = 10.0 Hz, 1H), 2.35–2.30 (m, 1H), 2.15 (t, *J* = 10.4 Hz, 2H), 2.12–2.07 (m, 1H), 1.62–1.52 (m, 1H), 1.46–1.37 (m, 1H); ESI-HRMS ([M + H]$^+$) calcd for $C_{24}H_{27}NO_4$ 394.2018, found 394.2016. For **19b**: mp 228–230 °C; $[\alpha]^{23}_D$= −81.5 ° (*c* 0.44, $CHCl_3$); ^{1}H NMR (400 MHz, $CDCl_3$): δ 7.86 (s, 1H), 7.85 (d, *J* = 2.4 Hz, 1H), 7.70 (d, *J* = 9.2 Hz, 1H), 7.19 (s, 1H), 7.15 (dd, *J* = 9.2 Hz, *J* = 2.4 Hz, 1H), 4.30 (d, *J* = 15.2 Hz, 1H), 4.09 (s, 3H), 4.08 (m, 1H), 4.04 (s, 3H), 4.00 (s, 3H), 3.55 (d, *J* = 15.6 Hz, 1H), 3.26–3.23 (m, 1H), 3.05 (dd, *J* = 16.4 Hz, *J* = 3.2 Hz, 1H), 2.83 (dd, *J* = 16.4 Hz, *J* = 10.0 Hz, 1H), 2.43 (dd, *J* = 12.0 Hz, *J* = 1.6 Hz, 1H), 2.41–2.35 (m, 1H), 1.98–1.94 (m, 1H), 1.90–1.85 (m, 2H), 1.69–1.61 (m, 1H); ESI-HRMS ([M + H]$^+$) calcd for $C_{24}H_{27}NO_4$ 394.2018, found 394.2022.

(14*R*/*S*,14a*S*)-11-Oxo-14-hydroxyl-cryptopleurine (20a/20b)

The preparation of the aldehyde was similar as for compounds **2a**/**2b**. At −78 °C under N_2, to a solution of LiHMDS (1.5 mL, 1.50 mmol) in THF was added methyl propiolate (91μL, 1.10 mmol) and the reaction mixture was stirred for 1 h. Then the aldehyde (~ 1 mmol) in 10 mL of THF was added dropwise over 5 min. Stirring was continued for 2 h before sat. NH_4Cl was added. The mixture was warned to rt and CH_2Cl_2 was used for extraction. After routine workup, the residue was dissolved in MeOH and subjected to catalytic hydrogenation using Pd/C (100 mg) at 50 psi for 2 h. The catalyst was filtered off and the solvent was evaporated under reduced pressure. Then the residue was dissolved in TFA/CH_2Cl_2 and stirred for 1 h before Et_3N (3 equiv.) and MeOH (15 mL) were added. The resulting mixture was refluxed for 2 h. Finally, the mixture was chromatographed using MeOH/CH_2Cl_2 to give an inseparable mixture of **20a** and **20b** (191 mg, 47%) as a white solid. ^{1}H NMR (400 MHz, $CDCl_3$): δ 7.91–7.84 (m, 3H), 7.24–7.17 (m, 2H), 5.88 (d, *J* = 17.2 Hz, 0.58H), 5.72 (d, *J* = 17.2 Hz, 0.34H), 4.53–4.42 (d, *J* = 18.0 Hz, 1H), 4.22 (m, 0.77 H), 4.11 (s, 3H), 4.05 (s, 3H), 4.00 (s, 3H), 3.93–3.88 (m, 0.79H), 3.77–3.73 (m, 1H), 3.38 (dd, *J* = 16.0 Hz, *J* = 2.8 Hz, 1H), 2.95 (m, 1H), 2.84–2.71 (m, 1H), 2.61–2.48 (m, 1H), 2.27–2.20 (m, 1H), 2.10–2.02 (m, 1H); ESI-HRMS ([M + H]$^+$) calcd for $C_{24}H_{25}NO_5$ 408.1811, found 408.1803.

(14*S*,14a*S*)-11-Oxo-14-hydroxycryptopleurine (21a) and (14*R*,14a*S*)-11-oxo-14-hydroxycryptopleurine (21b)

The mixture of **20a**/**20b** (84 mg, 0.21 mmol) was suspended in THF (20 mL), to which borane-methyl sulfide (1.0 mL, 1.00 mmol) was added. The reaction mixture was stirred overnight before MeOH (5 mL) was added and warmed to reflux for 0.5 h. The mixture was chromatographed using MeOH/CH_2Cl_2 to afford **21a** (14.4 mg) and **21b** (18.8 mg) as white solids. Yield: 41%. For **21a**: mp 136–138 °C; $[\alpha]^{23}_D$= −40.9° (*c* 0.23, $CHCl_3$); ^{1}H NMR (400 MHz, $CDCl_3$): δ 7.90–7.89 (m, 2H), 7.78 (d, *J* = 9.2 Hz, 1H), 7.29 (s, 1H), 7.19 (dd, *J*

= 8.8 Hz, *J* = 2.4 Hz, 1H), 4.47 (d, *J* = 15.6 Hz, 1H), 4.10 (s, 3H), 4.05 (s, 3H), 4.01 (s, 3H), 3.91 (br s, 1H), 3.67 (d, *J* = 15.6 Hz, 1H), 3.53 (dd, *J* = 16.4 Hz, *J* = 10.4 Hz, 1H), 3.24–3.21 (m, 1H), 2.98 (dd, *J* = 16.8 Hz, *J* = 4.0 Hz, 1H), 2.61–2.57 (m, 2H), 2.34–2.28 (m, 1H), 2.10–2.03 (m, 2H), 1.69–1.66 (m, 1H); ESI-HRMS ($[M + H]^+$) calcd for $C_{24}H_{27}NO_4$ 394.2018, found 394.2017. For **21b**: mp 239 °C (dec.); $[\alpha]^{23}_D$= −170.9° (*c* 0.11, $CHCl_3$); ^{1}H NMR (400 MHz, $CDCl_3$): δ 7.90 (s, 1H), 7.89 (d, *J* = 2.4 Hz, 1H), 7.77 (d, *J* = 9.2 Hz, 1H), 7.31 (s, 1H), 7.19 (dd, *J* = 9.2 Hz, *J* = 2.4 Hz, 1H), 4.47 (d, *J* = 15.6 Hz, 1H), 4.10 (s, 3H), 4.06 (s, 3H), 4.01 (s, 3H), 3.71–3.64 (m, 2H), 3.60 (dd, *J* = 16.4 Hz, *J* = 3.2 Hz, 1H), 3.22–3.19 (m, 1H), 2.96 (dd, *J* = 16.4 Hz, *J* = 9.2 Hz, 1H), 2.34–2.28 (m, 2H), 2.19–2.16 (m, 1H), 1.89–1.81 (m, 2H), 1.50–1.44 (m, 1H); ESI-HRMS ($[M + H]^+$) calcd for $C_{24}H_{27}NO_4$ 394.2018, found 394.2013.

(*R*,*E*)-*N*-Boc-3-(4-ethoxy-4-oxobut-2-enyl)-6,7,10-trimethoxy-3,4-dihydrodibenzo[*f*,*h*]isoquinoline (22)

To a solution of compound **10** (233 mg, 0.50 mmol) in CH_2Cl_2 (10 mL) was added $Ph_3P{=}CH_2CO_2Et$ (348 mg, 1 mmol) in one portion. The reation mixture was stirred at 40 °C for 5 h. After normal workup, the residue was chromatographed using EtOAc/hexane to give 238 mg of **22** as a light yellow foam in a yield of 89%. mp 173–175 °C; $[\alpha]^{23}_D$= 146.9° (*c* 0.13, $CHCl_3$); ^{1}H NMR (400 MHz, $CDCl_3$, peak broadened due to rotamers at r.t.): δ 7.93–7.78 (m, 3H), 7.28–7.22 (m, 2H), 7.03–6.83 (m, 1H), 5.91–5.78 (d, *J* = 15.6 Hz, 1H), 5.41–5.23 (m, 1H), 5.06–4.89 (m, 1H), 4.65–4.50 (d, *J* = 16.8 Hz, 1H), 4.16 (q, *J* = 7.2 Hz, 2H), 4.11 (s, 3H), 4.04 (s, 3H), 4.02 (s, 3H), 3.40–3.29 (dd, *J* = 16.0 Hz, *J* = 6.0 Hz, 1H), 3.09 (d, *J* = 16.4 Hz, 1H), 2.57–2.50 (m, 1H), 2.34 (br s, 1H), 1.53 (s, 9H), 1.27 (t, *J* = 7.2 Hz, 3H); ESI-HRMS ($[M + H]^+$) calcd for $C_{31}H_{37}NO_7$ 536.2648, found 536.2652.

(12*S*/13*S*,12*R*/13*R*,14a*S*)-11-Oxo-12,13-dihydroxycryptopleurine (23a/23b)

To a solution of amide **22** (238 mg, 0.44 mmol) in 15 mL of acetone and H_2O (8:1) was sequentially added OsO_4 (2.5wt% in *t*-BuOH, 0.05 mmol) and 4-methylmorpholine N-oxide (155 mg, 1.32 mmol). The reaction mixture was stirred at 50 °C for 6 h before excess $Na_2S_2O_3$ was added to quench the reaction. The mixture was extracted with CH_2Cl_2, washed with brine, and dried over Na_2SO_4. The solvent was then removed in vacuo, 10 mL of TFA in CH_2Cl_2 (1:1) was added, and the mixture was stirred for 0.5 h. After that, the solvent was evaporated and the trace of TFA was neutralized by Et_3N. The residue was stirred in 10 mL of MeOH and 0.2 mL of Et_3N for 2 h. Chromatography using MeOH/CH_2Cl_2 gave an inseparable mixture of **23a** and **23b** as a yellow solid (130 mg, yield: 67% over three steps, in about 5:4 ratio as indicated by NMR). ^{1}H NMR (400 MHz, $CDCl_3$): δ 7.92–7.84 (m, 3H), 7.27–7.17 (m, 2H), 6.00 (d, *J* = 17.2 Hz, 0.43H), 5.54 (d, *J* = 18.0 Hz, 0.56H), 4.62 (d, *J* = 18.0 Hz, 0.65H), 4.45 (d, *J* = 17.2 Hz, 0.51H), 4.24 (m, 0.65H), 4.11 (s, 3H), 4.07 (s, 3H), 4.02 (m, 4H), 3.77 (m, 0.71H), 3.38 (dd, *J* = 16.0 Hz, *J* = 3.2 Hz, 1H), 2.97 (dd, *J* = 16.4 Hz, *J* = 10.8 Hz, 1H), 2.67–2.64 (m, 1H), 2.41–2.31 (m, 1H), 2.00 (m, 1H); ESI-HRMS ($[M + H]^+$) calcd for $C_{24}H_{25}NO_6$ 424.1760, found 424.1757.

(12*S*,13*S*,14a*S*)-12,13-Dihydroxycryptopleurine (24a) and (12*R*,13*R*,14a*S*)-12,13-dihydroxycryptopleurine (24b)

Similar procedure as for compounds **21a** and **21b**. For **24a**: mp 225–227 °C; $[\alpha]^{23}_D$= −100.3° (*c* 0.10, $CHCl_3$); ^{1}H NMR (400 MHz, $CDCl_3$): δ 7.90 (s, 1H), 7.88 (d, *J* = 2.4 Hz, 1H), 7.76 (d, *J* = 9.2 Hz, 1H), 7.23 (s, 1H), 7.20 (dd, *J* = 9.2 Hz, *J* = 2.4 Hz, 1H), 4.48 (d, *J* = 15.6 Hz, 1H), 4.10 (s, 3H), 4.06 (s, 3H), 4.01 (s, 3H), 3.83–3.77 (m, 1H), 3.71–3.68 (m, 1H), 3.65–3.59 (m, 1H), 3.43 (dd, *J* = 11.2 Hz, *J* = 4.4 Hz, 1H), 3.16 (dd, *J* = 16.4 Hz, *J* = 3.2 Hz, 1H), 2.90 (dd, *J* = 16.4 Hz, *J* = 10.0 Hz, 1H), 2.57–2.52 (m, 1H), 2.38–2.33 (m, 1H), 2.30 (t, *J* = 10.4 Hz, 1H), 1.64 (q, *J* = 12.0 Hz, 1H); ESI-HRMS ($[M + H]^+$) calcd for $C_{24}H_{27}NO_5$

410.1967, found 410.1970. For **24b**: mp 246–248 °C; $[\alpha]^{23}_{D}$= −112.7° (*c* 0.15, $CHCl_3$); ^{1}H NMR (400 MHz, $CDCl_3$): δ 7.90 (s, 1H), 7.88 (d, *J* = 2.4 Hz, 1H), 7.76 (d, *J* = 9.2 Hz, 1H), 7.22 (s, 1H), 7.19 (dd, *J* = 9.2 Hz, *J* = 2.4 Hz, 1H), 4.37 (d, *J* = 15.2 Hz, 1H), 4.10 (s, 3H), 4.08 (m, 1H), 4.06 (s, 3H), 4.00 (s, 3H), 3.83 (br s, 1H), 3.77 (d, *J* = 15.6 Hz, 1H), 3.11 (dd, *J* = 12.0 Hz, *J* = 3.2 Hz, 1H), 3.04 (m, 1H), 2.93 (dd, *J* = 12.0 Hz, *J* = 1.6 Hz, 1H), 2.88–2.85 (m, 2H), 2.09–2.06 (m, 2H); ESI-HRMS ($[M + H]^+$) calcd for $C_{24}H_{27}NO_5$ 410.1967, found 410.1978.

(13*R*,14a*S*)-13-Ethyl-13-hydroxycryptopleurine (25)

To a solution of compound **12** (14 mg, 0.036 mmol) in THF was added EtMgBr (0.10 mL, 0.10 mmol) under N_2 at 0 °C. The resulting mixture was stirred for 1 h before sat. NH_4Cl was added to quench the reaction. CH_2Cl_2 was used for extraction. The organic layers were combined and washed with aq. $NaHCO_3$ and brine, and dried over Na_2SO_4. The solvent was removed in vacuo and the residue was chromatographed using MeOH/CH_2Cl_2 to give **25** (7.8 mg, 51%) as a light yellow solid. mp 208–210 °C; $[\alpha]^{23}_{D}$= −118.5° (*c* 0.11, $CHCl_3$); ^{1}H NMR (400 MHz, $CDCl_3$): δ 7.88 (s, 1H), 7.86 (d, *J* = 2.4 Hz, 1H), 7.78 (d, *J* = 8.8 Hz, 1H), 7.19 (s, 1H), 7.18 (dd, *J* = 8.8 Hz, *J* = 2.4 Hz, 1H), 4.46 (d, *J* = 15.2 Hz, 1H), 4.09 (s, 3H), 4.03 (m, 1H), 3.99 (s, 3H), 3.66 (d, *J* = 15.6 Hz, 1H), 3.12–3.08 (m, 1H), 3.01 (dd, *J* = 16.0 Hz, *J* = 2.4 Hz, 1H), 2.82 (dd, *J* = 16.0 Hz, *J* = 11.2 Hz, 1H), 2.75–2.69 (m, 2H), 1.96 (dt, *J* = 10.2 Hz, *J* = 2.8 Hz, 1H), 1.86 (dt, *J* = 11.2 Hz, *J* = 4.4 Hz, 1H), 1.72–1.68 (m, 1H), 1.59 (q, *J* = 7.6 Hz, 2H), 1.55 (m, 1H), 1.01 (t, *J* = 7.6 Hz, 3H); ESI-HRMS ($[M + H]^+$) calcd for $C_{26}H_{31}NO_4$ 422.2331, found 422.2349.

(13*S*,14a*S*)-13-Methoxycryptopleurine (26a) and (13*R*,14a*S*)-13-methoxycryptopleurine (26b)

To a solution of LiHMDS (0.30 mmol) in THF under Ar was added EtOAc (25 μl, 0.25 mmol) in 1 mL of THF at −78 °C, and the resulting mixture was stirred for 1 h before compound **10** (93 mg, 0.20 mmol) in 1 mL of THF was added slowly. The reaction mixture was stirred at −78 °C for about 2 h as indicated by TLC. Then sat. NH_4Cl was added and the mixture was extracted with CH_2Cl_2, dried over Na_2SO_4. After the Boc group was removed with TFA, the residue was stirred in Et_3N/MeOH for 2 h and the intermediate was purified through a short column using MeOH/CH_2Cl_2 as elutant. The solvent was evaporated and the residue was redissolved in THF, to which NaH (20 mg) was added. The reaction mixture was stirred for 0.5 h followed by addition of Me_2SO_4 before the temperature was warmed to 50 °C. The reaction was quenched as monitored by TLC (about 1 h) and after normal workup, the mixture was dried over Na_2SO_4. At last, the solvent was removed *in vacuo* and the residue was redissolved in THF, to which BMS (0.2 mL, 0.20 mmol) was added. The mixture was stirred overnight and MeOH was used to quench the reaction in reflux. The mixture was purified using MeOH/CH_2Cl_2 as elutant to give 7.2 mg of **26a** and 6.4 mg of **26b** as light yellow solids in 17% yield over five steps. For **26a**: mp 218–220 °C; $[\alpha]^{23}_{D}$= −83.8 ° (*c* 0.29, $CHCl_3$); ^{1} H NMR (400 MHz, $CDCl_3$): δ 7.91 (s, 1H), 7.89 (d, *J* = 2.4 Hz, 1H), 7.79 (d, *J* = 9.2 Hz, 1H), 7.26 (s, 1H), 7.19 (dd, *J* = 9.2 Hz, *J* = 2.4 Hz, 1H), 4.49 (d, *J* = 15.6 Hz, 1H), 4.10 (s, 3H), 4.06 (s, 3H), 4.01 (s, 3H), 3.60 (d, *J* = 15.6 Hz, 1H), 3.44 (s, 3H), 3.39–3.30 (m, 2H), 3.14 (dd, *J* = 16.4 Hz, *J* = 3.2 Hz, 1H), 2.94 (dd, *J* = 16.0 Hz, *J* = 10.4 Hz, 1H), 2.47–2.31 (m, 3H), 2.21–2.17 (m, 1H), 1.76–1.66 (m, 1H), 1.54–1.46 (m, 1H); ESI-HRMS ($[M + H]^+$) calcd for $C_{25}H_{29}NO_4$ 408.2175, found 408.2178. For **26b**: mp 115–117 °C; $[\alpha]^{23}_{D}$= −183.8° (*c* 0.08, $CHCl_3$); ^{1}H NMR (400 MHz, $CDCl_3$): δ 7.91 (s, 1H), 7.89 (d, *J* = 2.4 Hz, 1H), 7.79 (d, *J* = 9.2 Hz, 1H), 7.24 (s, 1H), 7.19 (dd, *J* = 9.2 Hz, *J* = 2.4 Hz, 1H), 4.45 (d, *J* = 15.2 Hz, 1H), 4.10 (s, 3H), 4.06 (s, 3H), 4.01 (s, 3H), 3.72 (d, *J* = 16.0 Hz, 1H), 3.69 (m, 1H), 3.40 (s, 3H), 3.09–3.01 (m, 2H), 2.89–2.78 (m, 2H), 2.74–2.67 (m, 1H), 2.31–2.26 (m, 1H), 2.09–2.04 (m, 1H), 1.98–1.89 (m, 1H), 1.71–1.64 (m, 1H); ESI-HRMS ($[M + H]^+$) calcd for $C_{25}H_{29}NO_4$ 408.2175, found 408.2169.

Supplementary Material

Refer to Web version on PubMed Central for supplementary material.

Acknowledgments

This study was supported by grant CA 17625 from National Cancer Institute awarded to K.H. Lee and grant DOH98-TD-G-111-007 from National Research Program for Genomic Medicine awarded to P.C. Yang. This study was also supported in part by the Cancer Research Center of Excellence (CRC) (DOH-100-TD-C-111-005).

ABBREVIATIONS

ATL	adult T-cell leukemia
BMS	borane dimethyl sulfide
dr	diastereomeric ratio
EDC•HCl	1-ethyl-3-(3-dimethyllaminopropyl)carbodiimide hydrochloride
HOBt	hydroxybenzotriazole
HTLV-1	human T-cell leukemia virus type 1
HUVEC	human umbilical vein endothelial cell
NMM	*N*-methylmorpholine
Py•SO_3	sulfur trioxide pyridine complex
LiHMDS	lithium bis(trimethylsilyl)amide (LiHMDS)

REFERENCES

1. (a) Gellert E. The indolizidine alkaloids. J. Nat. Prod. 1982; 45:50–73.(b) Li Z, Jin Z, Huang R. Isolation, total synthesis and biological activity of phenanthroindolizidine and phenanthroquinolizidine alkaloids. Synthesis. 2001; (16):2365–2378.(c) Chemler SR. Phenanthroindolizidines and phenanthroquinolizidines: promising alkaloids for anti-cancer therapy. Curr. Bioact. Compd. 2009; 5:2–19. [PubMed: 20160962]
2. NCI 60-cell assay results can be found. at http://dtp.nci.nih.gov/dtpstandard/dwindex/index.jsp
3. Gao W, Lam W, Zhong S, Kaczmarek C, Baker David C, Cheng Y-C. Novel mode of action of tylophorine analogs as antitumor compounds. Cancer Res. 2004; 64:678–688. [PubMed: 14744785]
4. (a) Huang MT, Grollman AP. Mode of action of tylocrebrine - effects on protein and nucleic-acid synthesis. Mol. Pharmacol. 1972; 8:538–550. [PubMed: 4343427] (b) Gupta RS, Siminovitch L. Mutants of CHO cells resistant to the protein synthesis inhibitors, cryptopleurine and tylocrebrine: genetic and biochemical evidence for common site of action of emetine, cryptopleurine, tylocrebrine, and tubulosine. Biochemistry. 1977; 16:3209–3214. [PubMed: 560858] (c) Gupta RS, Krepinsky JJ, Siminovitch L. Structural determinants responsible for the biological activity of (-)-emetine, (-)-cryptopleurine, and (-)-tylocrebrine: structure-activity relationship among related compounds. Mol. Pharmacol. 1980; 18:136–143. [PubMed: 7412757] (d) Dolz H, Vazquez D, Jimenez A. Quantitation of the specific interaction of [14a-3H]cryptopleurine with 80S and 40S ribosomal species from the yeast *Saccharomyces cerevisiae*. Biochemistry. 1982; 21:3181–3187. [PubMed: 7049239]
5. Cai XF, Jin X, Lee D, Yang YT, Lee K, Hong Y-S, Lee J-H, Lee JJ. Phenanthroquinolizidine alkaloids from the roots of *Boehmeria pannosa* potently inhibit hypoxia-inducible factor-1 in AGS human gastric cancer cells. J. Nat. Prod. 2006; 69:1095–1097. [PubMed: 16872154]
6. (a) Rao KN, Bhattacharya RK, Venkatachalam SR. Inhibition of thymidylate synthase and cell growth by the phenanthroindolizidine alkaloids pergularinine and tylophorinidine. Chem. Biol. Interact. 1997; 106:201–212. [PubMed: 9413547] (b) Rao KN, Bhattacharya RK, Veankatachalam SR. Inhibition of thymidylate synthase by pergularinine, tylophorinidine and deoxytubulosine.

Indian J. Biochem. Biophys. 1999; 36:442–448. [PubMed: 10844999] (c) Rao KN, Venkatachalam SR. Inhibition of dihydrofolate reductase and cell growth activity by the phenanthroindolizidine alkaloids pergularinine and tylophorinidine: the in vitro cytotoxicity of these plant alkaloids and their potential as antimicrobial and anticancer agents. Toxicol. In Vitro. 2000; 14:53–59. [PubMed: 10699361]

7. Suffness, M.; Douros, J. Anticancer Agents Based on Natural Product Models. Academic Press; p. 465-487.
8. Gao W, Bussom S, Grill SP, Gullen EA, Hu Y-C, Huang X, Zhong S, Kaczmarek C, Gutierrez J, Francis S, Baker DC, Yu S, Cheng Y-C. Structure-activity studies of phenanthroindolizidine alkaloids as potential antitumor agents. Bioorg. Med. Chem. Lett. 2007; 17:4338–4342. [PubMed: 17531481]
9. (a) Wei L, Shi Q, Bastow Kenneth F, Brossi A, Morris-Natschke Susan L, Nakagawa-Goto K, Wu T-S, Pan S-L, Teng C-M, Lee K-H. Antitumor agents 253. Design, synthesis, and antitumor evaluation of novel 9-substituted phenanthrene-based tylophorine derivatives as potential anticancer agents. J. Med. Chem. 2007; 50:3674–3680. [PubMed: 17585747] (b) Yang X, Shi Q, Liu YN, Zhao G, Bastow KF, Lin JC, Yang SC, Yang PC, Lee KH. Antitumor agents 268. Design, synthesis, and mechanistic studies of new 9-substituted phenanthrene-based tylophorine analogues as potent cytotoxic agents. J. Med. Chem. 2009; 52:5262–5268. [PubMed: 19645447]
10. Yang XM, Shi Q, Bastow KF, Lee KH. Antitumor agents. 274. A new synthetic strategy for E-ring SAR study of antofine and cryptopleurine analogues. Org. Lett. 2010; 12:1416–1419. [PubMed: 20196574]
11. Yang X, Shi Q, Yang S-C, Chen C-Y, Yu S-L, Bastow KF, Morris-Natschke SL, Wu P-C, Lai C-Y, Wu T-S, Pan S-L, Teng C-M, Lin J-C, Yang P-C, Lee K-H. Antitumor agents 288: Design, synthesis, SAR, and biological studies of novel heteroatom-incorporated antofine and cryptopleurine analogues as potent and selective antitumor agents. J. Med. Chem. 2011; 54:5097–5107. [PubMed: 21668000]
12. Cooper LC, Prinsloo E, Edkins AL, Blatch GL. Hsp90α/β associates with the GSK3β/axin1/phospho-β-catenin complex in the human MCF-7 epithelial breast cancer model. Biochem. Biophys. Res. Commun. 2011; 413:550–554. [PubMed: 21925151]
13. Kurashina R, Ohyashiki JH, Kobayashi C, Hamamura R, Zhang Y, Hirano T, Ohyashiki K. Anti-proliferative activity of heat shock protein (Hsp) 90 inhibitors via β-catenin/TCF7L2 pathway in adult T cell leukemia cells. Cancer Lett. (Shannon, Irel.). 2009; 284:62–70.

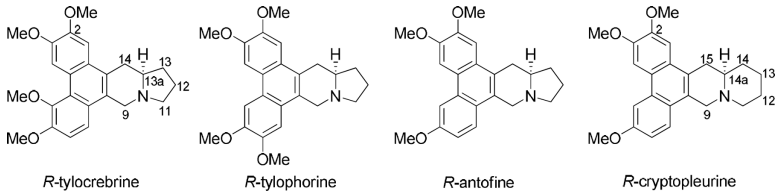

Figure 1.
Representatives of phenanthroindolizidines and phenanthroquinolizidines

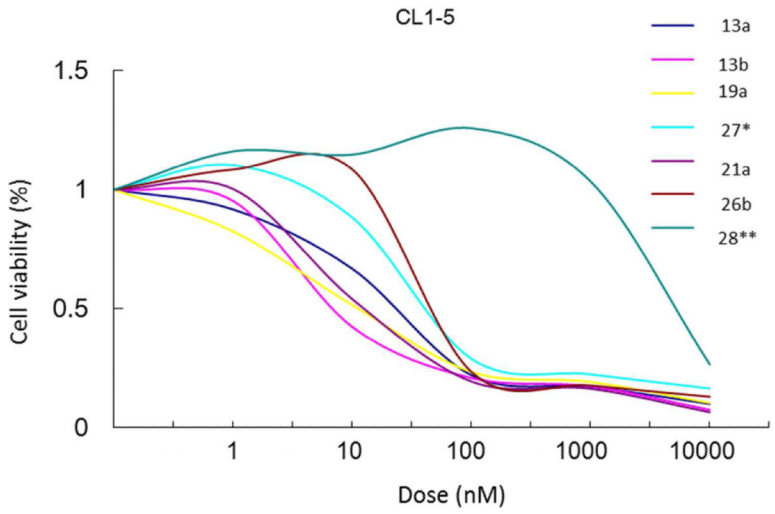

Figure 2.

Inhibitory effect of selected compounds on CL1-5 NSCLC cell proliferation. Cell viability was determined by SRB assay. *Compound **16** in Ref. 11. ** 8-membered E-ring analog.

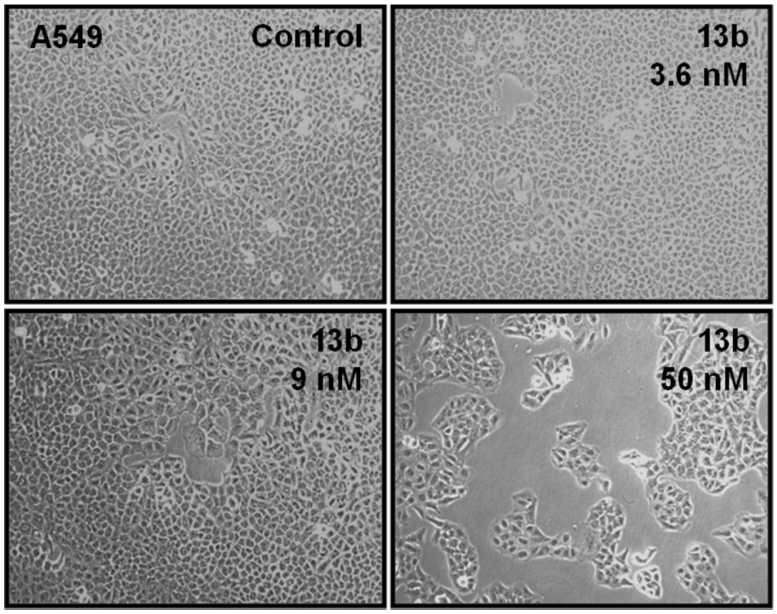

Figure 3.
Morphological effect of **13b** on A549 cells.

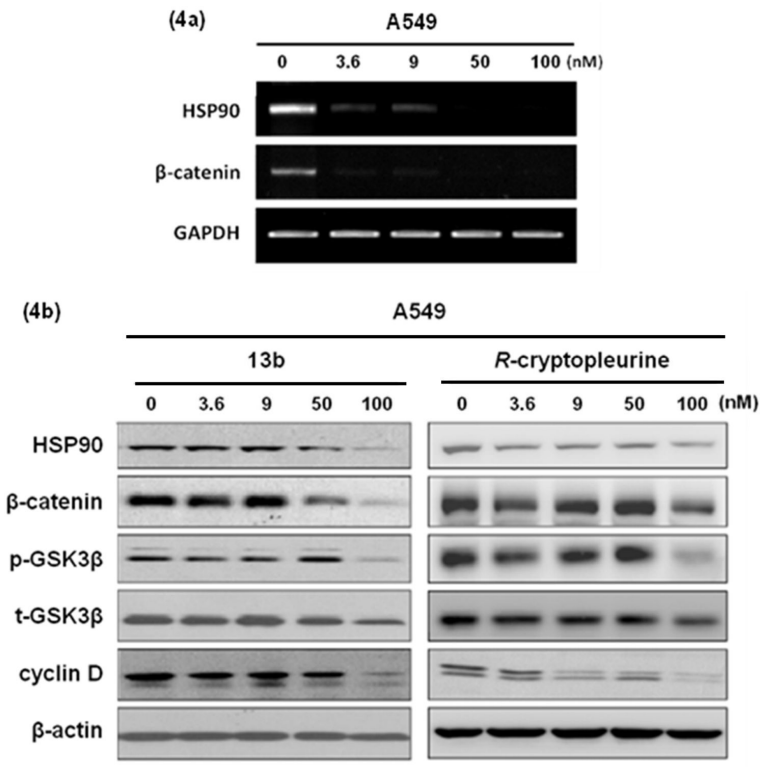

Figure 4.

(a) Inhibition of HSP90 and β-catenin by **13b** through RT-PCR analysis. (b) Western blot analysis of **13b** in A549 cells for 48 h. Whole cell extracts were prepared and used for immunoblot analysis using the indicated antibodies.

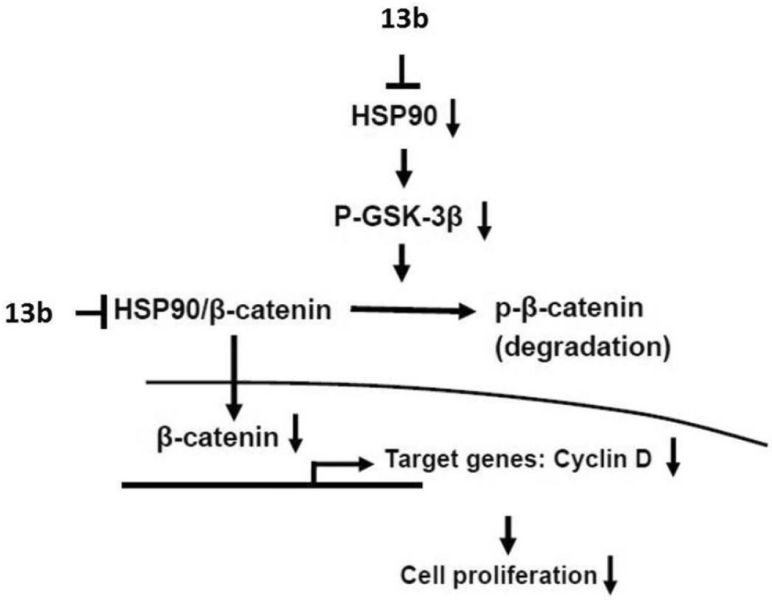

Figure 5.
Proposed pathways involved in **13b**-induced cytotoxic effect in A549 cells modified from the MetaCore databases.

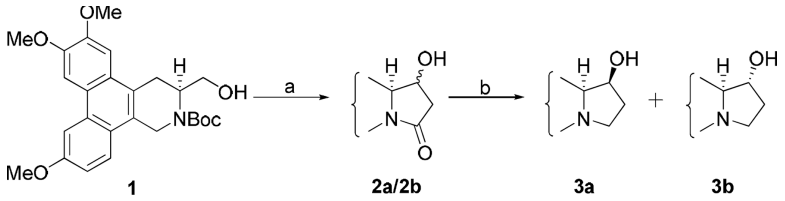

Scheme 1.

Reagents and conditions: (a) i) $Py{\cdot}SO_3$, DMSO, Et_3N, CH_2CI_2; ii) LiHMDS, EtOAc, −78 °C, THF; iii) TFA, CH_2CI_2; iv) Et_3N, MeOH, reflux, 57% over four steps (b) $LiAIH_4$, THF, 70%

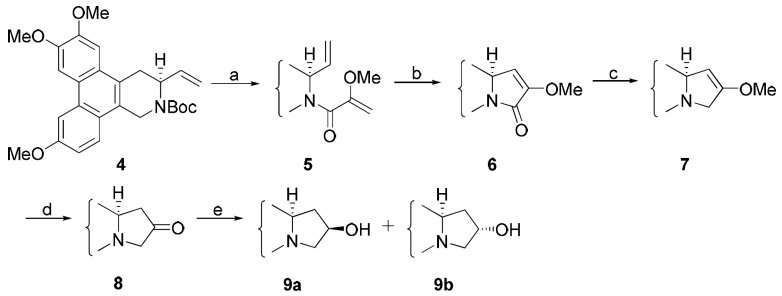

Scheme 2.

Reagents and conditions: (a) i) TFA, CH_2CI_2; ii) 2-methylacrylic acid, EDC, HOBt, DMF, 83% over two steps (b) Grubb's 2nd generation catalyst, CH_2CI_2, 88% (c) $LiAIH_4$, THF, 69% (d) HCI, THF, reflux, 68% (e) $NaBH_4$, MeOH, r.t., 80%, **9a/9b** = 5/3

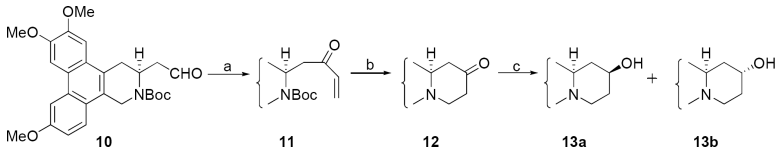

Scheme 3.

Reagents and conditions: (a) i) vinylmagnesium bromide, THF, 0 °C ii) Dess-Martin reagent, CH_2Cl_2, 57% over two steps (b) i) TMSI, CH_3CN, 0 °C; ii) Cs_2CO_3, MeOH, reflux, 63% over two steps (c) $NaBH_4$, MeOH, **13a:13b**= 3:7, 80% or L-selectride, THF, 0°C, **13a: 13b** = 1:9, 90%

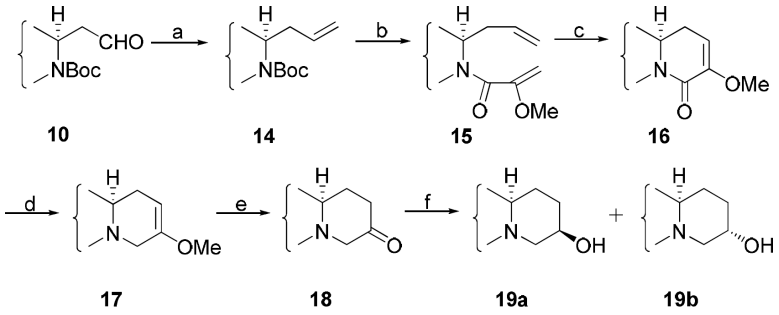

Scheme 4.

Reagents and conditions: (a) $Ph_3P{=}CH_2Br$, n-BuLi, THF, 85% (b) i) TFA, CH_2CI_2; ii) 2-methoxyacrylicacid, EDC, HOBt, DMF, 77% (c) Grubb's 2nd generation catalyst, CH_2CI_2, reflux, 65% (d) $LiAIH_4$, THF, 70% (e) HCI, THF, reflux, 80% (f) $NaBH_4$, MeOH, **19a:19b** = 4:1,73% or L-selectride, THF, 0°C, **19a** (80%), **19b** (0%)

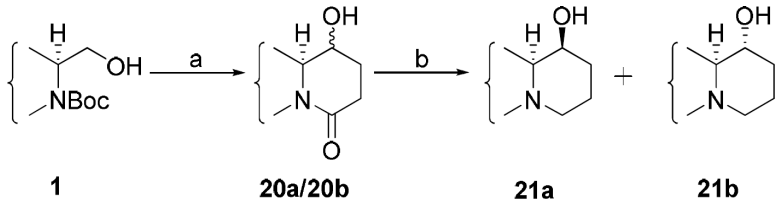

Scheme 5.

Reagents and conditions: (a) i) $Py{\cdot}SO_3$, DMSO, Et_3N, CH_2CI_2; ii) LiHMDS, methyl propiolate, −78 °C, THF; iii) Pd/C, H_2, MeOH; iv) TFA, CH_2CI_2; v) Et_3N, MeOH, reflux, 47% over five steps (b) BMS, THF, 41%

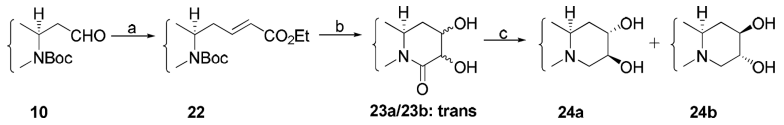

Scheme 6.

Reagents and conditions: (a) $Ph_3P{=}CH_2CO_2Et$, THF, 89% (b) i) OSO_4, NMO, Acetone/ H_20=8/1, overnight; ii) TFA, CH_2CI_2; iii) TEA, MeOH, reflux, 67% over three steps (c) BMS, THF, 37%

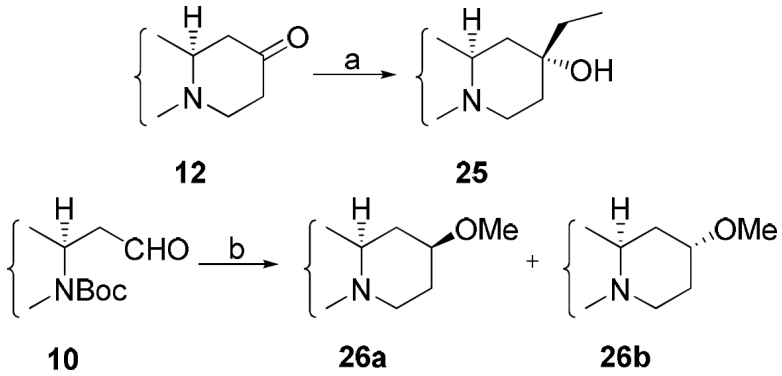

Scheme 7.

Reagents and conditions: (a) EtMgBr, THF, 0 °C, 51% (b) i) LiHMDs, ethyl acetate, THF, −78 °C; ii) TFA, CH_2CI_2; iii) MeOH, Et_3N; iv) Me_2SO_4, NaH, THF; v) BMS, THF, 17% over five steps

Table 1

IC_{50} values of hydroxylated *R*-antofine analogs

Cmpd	E-ring oxygenation	IC_{50} (μM)				Predicted C.brain/C. blood
		A549	DU145	KB	KBvin	
3a	13*R*-OH	2.81 ± 0.42	3.20 ± 0.49	1.83 ± 0.36	3.42 ± 0.38	0.059
3b	13*S*-OH	0.27 ± 0.035	0.85 ± 0.094	0.50 ± 0.077	0.64 ± 0.080	0.059
7	C13-OMe, Δ12–13	5.97 ± 0.84	10.30 ± 2.02	12.00 ± 2.18	2.64 ± 0.35	0.044
8	C12, C=O	0.29 ± 0.051	0.71 ± 0.083	0.50 ± 0.064	0.43 ± 0.052	0.334
9a	12*R*-OH	0.61 ± 0.087	0.70 ± 0.078	0.78 ± 0.085	0.64 ± 0.081	0.062
9b	12*S*-OH	2.27 ± 0.40	1.80 ± 0.39	1.81 ± 0.23	2.21 ± 0.32	0.062
***R*-anto-fine**	--	0.022 ± 0.007	0.025 ± 0.005	0.036 ± 0.008	0.025 ± 0.007	0.980

Table 2

IC_{50} values of new E-ring mono-hydroxylated analogs of *R*-cryptopleurine

Cmpd	E-ring oxygenation	IC_{50} (μM)					Predicted C.brain/C.blood
		A549	DU145	KB	KBvin	SKBR3	
12	C13, C=O	28 ± 9	45 ± 10	50 ± 9	43 ± 11	-	0.028
13a	13*S*-OH	72 ± 13	59 ± 12	43 ± 10	78 ± 16	295 ± 41	0.059
13b	13*R*-OH	22 ± 5	11 ± 4	23 ± 4	25 ± 7	72 ± 18	0.059
18	C12, C=O	910 ± 140	1700 ± 210	734 ± 110	1479 ± 220	3340 ± 420	0.078
19a	12*R*-OH	82 ± 18	66 ± 14	33 ± 8	45 ± 15	348 ± 40	0.128
19b	12*S*-OH	2510 ± 360	2250 ± 330	2250 ± 370	3070 ± 290	6440 ± 760	0.128
21a	14*S*-OH	10 ± 3	33 ± 10	25 ± 8	25 ± 8	-	0.123
21b	14*R*-OH	69 ± 10	200 ± 32	300 ± 39	120 ± 26	-	0.123
***R*-crypto-pleurine**	--	1.38 ± 0.56	1.59 ± 0.53	1.51 ± 0.33	1.91 ± 0.63 (HCT-8)	-	0.281

Table 3

Antiproliferative activity of new E-ring dihydroxylated analogs of *R*-cryptopleurine

Cmpd	E-ring oxygenation	IC_{50} (nM)				Predicted C.brain/C.blood
		A549	DU145	KB	KBvin	
24a	12*S*,13*S*-OH	550 ± 67	600 ± 93	840 ± 120	2170 ± 350	0.068
24b	12*R*,13*R*-OH	14480 ± 1540	1709 ± 260	17520 ± 1660	12560 ± 1350	0.068
***R*-cryptopleurine**	--	1.38 ± 0.56	1.59 ± 0.53	1.51 ± 0.33	1.91 ± 0.63 (HCT-8)	0.281

Table 4

IC_{50} values of new analogs **25, 26a,** and **26b**

Cmpd	E-ring oxygenation	IC_{50} (nM)				Predicted C.brain/C.blood
		A549	DU145	KB	KBvin	
25	13*R*-OH, Et	990 ± 82	770 ± 85	920 ± 88	870 ± 96	0.174
26a	13*S*-OMe	7110 ± 530	3570 ± 430	5240 ± 650	3690 ± 410	0.042
26b	13*R*-OMe	25 ± 6	56 ± 14	100 ± 22	66 ± 12	0.042
***R*-cryptopleurine**	--	1.38 ± 0.56	1.59 ± 0.53	1.51 ± 0.33	1.91 ± 0.63 (HCT-8)	0.281

Table 5

Inhibitory effects of **13b** and *R*-cryptopleurine on human NSCLC cell lines

	IC_{50} (nM)		
Cell line	**13b**	***R*-cryptopleurine**	***S*-oxa-cryptopleurine**
CL1–0	58.4 ± 0.02	5 ± 0.02	-
CL1–5	8.7 ± 0.02	1.8 ± 0.01	-
A549	9 ± 0.02	1.9 ± 0.11	40 ± 6
PC9	8.2 ± 0.03	5.5 ± 0.03	-
PC9IR	43.2 ± 0.01	6.8 ± 0.01	-
MRC-5	98 ± 10	14 ± 2	252 ± 24

Table 6

Identification of genes affected by **13b**

Pathway	Genes	*P*-Value
Development Hedgehog Signaling	Up-regulation: ubiquitin Down-regulation: HSP90, SAP18, CDK11, β-catenin, Casein kinase I, Skp2/TrCP/FBXW, PKA-cat (cAMP-dependent), DYRK2	5.423E-07
Cell adhesion plasma signaling	Down-regulation: Fibronectin, PI3K cat. Class IA, XIAP, PLAU (UPA), FRS2, PI3K reg. class IA, Collagen IV	8.889E-06
Transport clathrin-coated vesicle cycle	Down-regulation: Myosin Vb, Rabaptin-5, Syntazin 7, PLEKHA8 (FAPP2), SNAP-25, Eps 15, VTI1B, EEA1, PECALM	2.284E-05